

Low-overhead Joint Channel Estimation and Data Detection in ZP-OTFS System

Omid Abbassi Aghda, Mohammad Javad Omid, Hamid Saeedi-Sourck

Abstract— High pilot overhead and peak-to-average power ratio (PAPR) are challenging issues in channel estimation for orthogonal time frequency space (OTFS) systems. ZP-OTFS is a modified OTFS system where multiple rows along the delay axis are zero. We propose a two-step channel estimation method for the ZP-OTFS system. The proposed method inserts pilot sequences in the zero bins of the ZP-OTFS system, resulting in low overhead and PAPR. Our simulation results demonstrate the effectiveness of the proposed method and show that it outperforms embedded pilot estimation in terms of normalized mean square error (NMSE) at the same bit error rate (BER).

Index Terms—Channel estimation, delay-Doppler domain, OTFS, PAPR, sparse recovery.

I. INTRODUCTION

RELIABLE communication is essential in high-mobility environments for the 6th generation of wireless telecommunication systems. However, in such environments, orthogonal frequency division multiplexing is not effective due to a high Doppler shift, which results in high inter-carrier interference and degrades its performance. To address this issue, a new modulation technique called orthogonal time frequency space (OTFS) was proposed in [1]. OTFS multiplexes information symbols into the Delay-Doppler (DD) domain, where each information symbol spreads over the entire time-frequency (TF) domain. This technique enables full channel diversity to be exploited. The DD domain is the symplectic finite Fourier transform of the TF domain [1]. Despite the advantages of OTFS, data detection and channel estimation remain challenging issues that need to be addressed.

Data detection in OTFS systems is computationally expensive, especially for conventional methods such as zero-forcing (ZF) and minimum mean square error (MMSE). To address this issue, a low-complexity linear MMSE (LMMSE) detection method was proposed in [2], which exploits the structure of the delay-doppler (DD) channel matrix to reduce detection complexity. Additionally, the message passing (MP) algorithm has been used in [3] for data detection, which has significantly lower computational complexity compared to MMSE and ZF detectors. The MP detector takes advantage of the sparsity of the DD channel matrix. However, MP complexity depends on the frame size, the number of channel taps in the DD domain, and the constellation size of the quadrature amplitude modulation symbols, which can limit its practicality.

To further reduce detection complexity, the authors in [4] proposed a delay-time (DT) maximal ratio combining (MRC) detector for use in OTFS systems. The MRC detector has significantly less computational complexity compared to MP and LMMSE detectors since its complexity only depends on

the frame size and the maximum delay-spread of the channel. Furthermore, the MRC detector improves the signal-to-noise ratio (SNR) of the received signal, resulting in a lower bit error rate (BER). However, using the MRC detector requires a modified version of OTFS, named ZP-OTFS, where multiple rows along the delay axis are zero. While this zero-padding technique can be useful for inserting pilot symbols for channel estimation, it also imposes high overhead on the system, which is a significant disadvantage of ZP-OTFS.

Therefore, in this paper, we propose a two-step channel estimation method for ZP-OTFS systems that addresses this disadvantage by inserting pilot sequences in zero bins. The proposed method imposes less overhead and peak-to-average power ratio (PAPR) on the system compared to the conventional estimation method in OTFS. To the best of our knowledge, there is no further research on the channel estimation in ZP-OTFS systems. Our simulation results demonstrate that our two-step method outperforms embedded pilot (EP) estimation in normalized mean square error (NMSE) with the same BER.

Channel estimation is a crucial step in wireless communication systems as the detector's performance heavily relies on the accuracy of the estimated channel state information (CSI). In [5], the EP method was proposed to estimate CSI in OTFS. The EP method has low estimation error as it leverages the sparse nature of the DD channel representation, and the detection of channel taps is threshold-based, resulting in low computational cost. However, the EP scheme suffers from a high peak-to-average power ratio (PAPR) as the power of the pilot impulse in the DD domain increases. To address this issue, we propose spreading the pilot in the zero bins, resulting in much less PAPR. Additionally, the EP scheme imposes high pilot overhead on the OTFS system due to the guards separating the single pilot impulse from the data to avoid pilot contamination. To mitigate this overhead and exploit the sparse representation of the wireless channel in the DD domain, a channel estimation method based on the sparse recovery algorithm was investigated in [6]. Although this method outperforms the EP channel estimation, it incurs higher total power dedicated to pilot sequences, which could be burdensome. Our proposed estimation method inserts pilot sequences in the zero bins of the ZP-OTFS system, which does not impose additional overhead on the ZP-OTFS system and has less overhead compared to the EP scheme. Moreover, we use the sparse recovery algorithm to estimate CSI.

In the pursuit of increasing spectral efficiency, a superimposed DD domain channel estimation was proposed in [7]. This method assumes no pilot overhead for the system, and pilots and data are superimposed in each DD bin. An iterative

method is used at the receiver for joint channel estimation and data detection to cancel out pilot interference. However, this method assumes that the receiver has prior knowledge of the delay and Doppler of each channel coefficient, which makes it applicable only for the doubly-under-spread channel. Additionally, the covariance matrix of CSI is known at the receiver. In contrast, our proposed method estimates the delay and Doppler of each tap using a sparse recovery algorithm and assumes the covariance matrix of CSI is unknown at the receiver.

This paper presents a joint channel estimation and data detection method for the ZP-OTFS system, which offers several advantages including **i)** increased spectral efficiency, **ii)** improved power efficiency, **iii)** utilization of MRC detector's superiority over other detection methods, and **iv)** utilization of time-domain samples to estimate CSI without the need to transform the received signal into the DD domain.

The paper is structured as follows: Section II outlines the system design of the proposed method, while Section III describes the joint channel estimation and data detection process. In Section IV, simulation results of the proposed method are presented and compared with the EP method. Finally, Section V concludes the paper.

Notation: boldface upper case (**A**) for matrices, boldface lower case (**a**) for vectors, regular lower case (*a*) for scalars, $(\cdot)^H$ for Hermitian operator, $\text{vec}(\mathbf{A})$ vectorizes the matrix **A** by stacking its columns under each other, $\text{vec}^{-1}(\mathbf{a})$ unvectorize the vector **a**, \otimes for Kronecker product, \mathbf{F}_N for N -point DFT matrix, $\lfloor \cdot \rfloor$ and $\lfloor \cdot \rfloor_M$ are floor and modulo- M operator, respectively.

II. SYSTEM DESIGN

In the ZP-OTFS transceiver, the DD domain is divided into M and N bins along the delay and Doppler axes, respectively. The l^{th} delay bin ($l = 0, 1, \dots, M-1$) corresponds to a delay of $\tau = \frac{l}{M\Delta f}$, while the k^{th} Doppler bin ($k = 0, 1, \dots, N-1$) corresponds to a Doppler shift of $\nu = \frac{k}{NT_s}$, where Δf is the sub-carrier spacing. The available bandwidth is $B = M\Delta f$, while $T = NT_s$ is the frame duration, where T_s is the ZP-OTFS sub-symbol duration, and $T_s\Delta f = 1$.

A. The Transmitter

The signal transmitted in the DD domain is depicted in Fig. 1a, where both information and pilot symbols are arranged. The transmitted signal in the DD domain can be represented by the matrix $\mathbf{X} = \mathbf{X}_d + \mathbf{X}_p \in \mathbb{C}^{M \times N}$. In ZP-OTFS, the last l_{ZP} rows of the data matrix \mathbf{X}_d are zero, and the first $M - l_{ZP}$ rows carry information symbols, with an average power of one. To utilize all the available DD resources, the last l_{ZP} rows of the pilot matrix \mathbf{X}_p consist of pilot symbols, generated from the $\mathcal{N}(0, 1)$ distribution, while the rest of the rows are zero. As a result, the average power of the transmitted signal is also one.

As shown in Fig. 1c, the time-domain signal **s** can be obtained as the inverse discrete Zak transform (IDZT) of the DD-domain signal **X**

$$\mathbf{s} = \mathbf{s}_d + \mathbf{s}_p = \text{IDZT}(\mathbf{X}) = \text{vec}(\mathbf{X}\mathbf{F}_N^H) = (\mathbf{F}_N^H \otimes \mathbf{I}_M)\mathbf{x}, \quad (1)$$

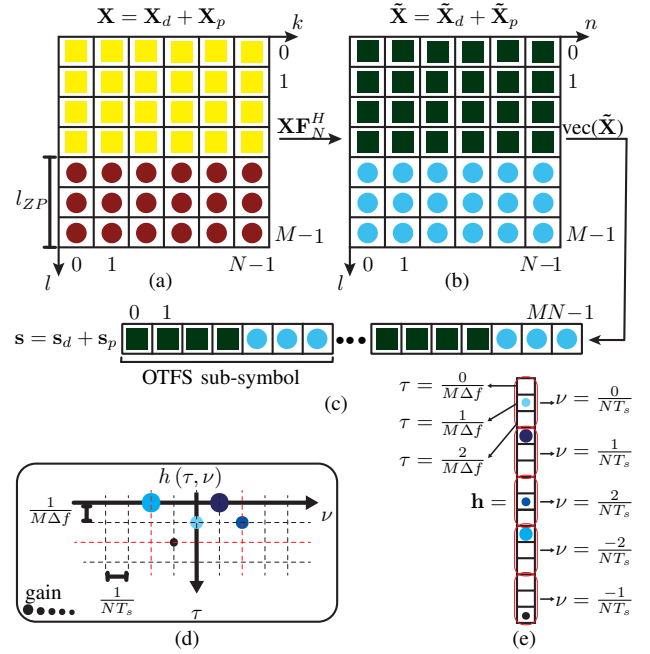


Fig. 1. transmitter system design and channel representation: (a) the DD signal **X**, (b) the DT signal $\tilde{\mathbf{X}}$, (c) the time signal **s**, (d) the DD channel $h(\tau, \nu)$, (e) the channel vector **h**. ■: DD data, ●: DD pilot, ■: DT data, ●: DT pilot

where $\mathbf{s} \in \mathbb{C}^{MN \times 1}$ and $\mathbf{x} = \text{vec}(\mathbf{X}) \in \mathbb{C}^{MN \times 1}$. To avoid inter-frame interference, a cyclic prefix (CP) is added to the beginning of **s**. The DT representation of the transmitted signal is defined as $\tilde{\mathbf{X}} = \mathbf{X}\mathbf{F}_N^H$, as shown in Fig. 1b. Additionally, $\mathbf{s}_d = \text{IDZT}(\mathbf{X}_d)$ and $\mathbf{s}_p = \text{IDZT}(\mathbf{X}_p)$ represent the time-domain data and pilot vectors, respectively, since IDZT is a linear transformation.

B. Channel Effect

The DD domain channel representation is shown in Fig. 1d, along with the mathematical expression of the DD channel given by $h(\tau, \nu) = \sum_{i=1}^Q h_i \delta(\tau - \tau_i, \nu - \nu_i)$. Here, $\{h_i\}_{i=1}^Q$ represents the channel coefficients and $Q = (l_{max} + 1)(2k_{max} + 1)$, where l_{max} and k_{max} denote the maximum delay and Doppler spread of the channel, respectively. The sparsity order of the DD channel is given by the ratio of non-zero channel coefficients P to Q . After removing the CP, the input-output relation is described by

$$\mathbf{r} = \mathbf{H}\mathbf{s} + \mathbf{w} = \mathbf{H}\mathbf{s}_d + \mathbf{H}\mathbf{s}_p + \mathbf{w} \quad (2)$$

where $\mathbf{w} \in \mathbb{C}^{MN \times 1}$ is the noise vector, $\mathbf{r} \in \mathbb{C}^{MN \times 1}$ is the time domain received signal, and $\mathbf{H} \in \mathbb{C}^{MN \times MN}$ is the time domain channel matrix [8]. The channel matrix **H** is formulated as shown in (3), where $\mathbf{\Pi} \in \mathbb{C}^{MN \times MN}$ is the standard permutation matrix, $\mathbf{\Delta} = \text{diag}(z^0, z^1, \dots, z^{MN-1}) \in \mathbb{C}^{MN \times MN}$ is the diagonal Doppler matrix, and $z = e^{j2\pi/(MN)}$ [9].

$$\mathbf{H} = \sum_{i=1}^Q h_i \mathbf{\Pi}^{l_i} \mathbf{\Delta}^{k_i} \quad (3)$$

By substituting (3) into (2), we obtain (4), which represents the input-output relation of the channel in the time domain.

Here, $\Psi_i = \Pi^{l_i} \Delta^{k_i} \mathbf{s} \in \mathbb{C}^{MN \times 1}$, $\mathbf{h} \in \mathbb{C}^{Q \times 1}$ represents the channel vector, and $\Psi = \Psi_d + \Psi_p \in \mathbb{C}^{MN \times Q}$ is the time domain signal matrix.

$$\mathbf{r} = [\Psi_1, \Psi_2, \dots, \Psi_Q] \mathbf{h} + \mathbf{w} = \Psi \mathbf{h} + \mathbf{w} = \Psi_d \mathbf{h} + \Psi_p \mathbf{h} + \mathbf{w} \quad (4)$$

Fig. 1e shows how to form \mathbf{h} from $h(\tau, \nu)$, where the i^{th} element of \mathbf{h} corresponds to h_i , and its delay and Doppler are $l_i = \lfloor i - 1 \rfloor_{l_{max}+1}$ and k_i as described by (5)

$$k_i = \begin{cases} \lfloor \frac{i-1}{l_{max}+1} \rfloor, & \text{if } \lfloor \frac{i-1}{l_{max}+1} \rfloor \leq k_{max}, \\ \lfloor \frac{i-1}{l_{max}+1} \rfloor - (2k_{max} + 1), & \text{if } \lfloor \frac{i-1}{l_{max}+1} \rfloor > k_{max}, \end{cases} \quad (5)$$

respectively. Finally, the paper proposes estimating the channel vector \mathbf{h} using the orthogonal matching pursuit (OMP) algorithm, which can be applied to (4).

C. Receiver

As depicted in Fig. 2a and Fig. 2b, the received signal can be represented in the time domain as $\mathbf{r} = \mathbf{r}_d + \mathbf{r}_p$, where \mathbf{r}_d and \mathbf{r}_p are the channel-effected data and pilot signals, respectively. To obtain the corresponding DD domain representation, we apply an N -point Discrete Fourier Transform (DFT) to $\tilde{\mathbf{Y}}$ along the time axis, yielding $\mathbf{Y} = \tilde{\mathbf{Y}} \mathbf{F}_N$, where $\tilde{\mathbf{Y}} = \text{vec}^{-1}(\mathbf{r})$ is the DT representation of the received signal. This approach has been previously described in [4].

In this work, we estimate the channel impulse response \mathbf{h} using \mathbf{r} , and then apply MRC detector to the received signal in the DT domain. Specifically, we perform a two-step channel estimation and data detection to obtain an enhanced estimate of the \mathbf{h} and transmitted data.

III. JOINT CHANNEL ESTIMATION AND DATA DETECTION

This paper proposes a two-step approach for channel estimation and data detection. In the first step, a coarse estimate of the channel is obtained. Then, interference cancellation is performed, followed by the use of a Maximum Ratio Combining (MRC) detector for detection. In the second step, the detected data and pilot sequences are jointly utilized as pilot to accurately estimate the channel.

Overall, this proposed approach can improve the accuracy of channel estimation and enhance the reliability of data detection, which is crucial for the reliable operation of wireless communication systems.

A. First Step

To estimate the CSI, the entries in \mathbf{r} without data interference are utilized. Hence, we rewrite (4) as (6), where $\mathbf{r}'_p \in \mathbb{C}^{N \times 1}$ denotes the pilot effect vector, $\mathbf{w}' \in \mathbb{C}^{N \times 1}$ represents the noise vector, and $\Psi'_p \in \mathbb{C}^{N \times Q}$ is the time-domain pilot matrix. The vector \mathbf{r}'_p is illustrated in Fig. 2c.

$$\mathbf{r}'_p = \Psi'_p \mathbf{h} + \mathbf{w}' \quad (6)$$

To estimate the channel vector $\hat{\mathbf{h}}$, we perform OMP on (6). To detect data, we cancel out the pilot effect of the received signal using

$$\mathbf{r}_d = \mathbf{r} - \Psi_p \hat{\mathbf{h}} = \Psi_d \mathbf{h} + \Psi_p (\mathbf{h} - \hat{\mathbf{h}}) + \mathbf{w}, \quad (7)$$

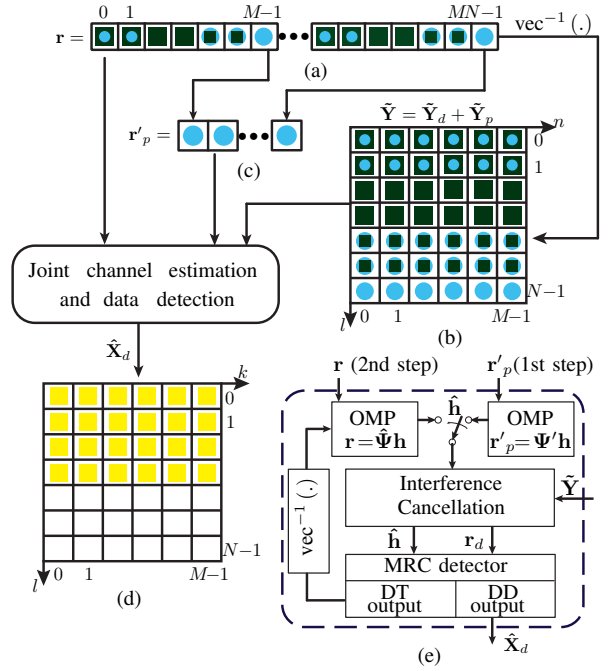


Fig. 2. the block diagram of the proposed algorithm at the receiver: (a) the time vector \mathbf{r} , (b) the pilot effect vector \mathbf{r}'_p , (c) the DT signal $\tilde{\mathbf{Y}}$, (d) the DD data signal \mathbf{Y} , (e) joint channel estimation and data detection algorithm. ■: DD data, ●: DD pilot, ■: contaminated pilot by data, ■: contaminated data by pilot

where $\mathbf{r}_d \in \mathbb{C}^{MN \times 1}$ denotes the received data vector without pilot effect. The detected data vector $\hat{\mathbf{x}}_d$ is obtained using the MRC detector with inputs $\hat{\mathbf{h}}$ and \mathbf{r}_d . Here, $\hat{\mathbf{s}}_d$ and $\hat{\Psi}_d$ are the time-domain vector and matrix of the detected data, respectively.

Note that the term $\Psi_p (\mathbf{h} - \hat{\mathbf{h}})$ in (7) represents the interference that remains due to the channel estimation error. To reduce this interference, a second step is necessary to obtain an accurate estimate of the channel vector, resulting in improved detection performance.

B. Second Step

In this step, the pilot sequences and detected data from the first step are jointly used as pilot to accurately estimate the channel and reduce detection errors. To achieve this, we rewrite (4) as

$$\mathbf{r} = (\Psi_p + \hat{\Psi}_d) \mathbf{h} + (\Psi_d - \hat{\Psi}_d) \mathbf{h} + \hat{\mathbf{w}} = (\Psi_p + \hat{\Psi}_d) \mathbf{h} + \hat{\mathbf{w}}, \quad (8)$$

where the term $\hat{\Psi} = \Psi_p + \hat{\Psi}_d$ is considered as the joint pilot. Unlike the first step, this approach uses all the entries of \mathbf{r} to estimate the channel, including those with data interference. The channel vector is then estimated by performing the OMP algorithm on (8).

To detect data, we remove the pilot contamination from the received signal using (7), and employ the MRC detector to detect the data matrix $\hat{\mathbf{X}}_d$. The detected data is depicted in Fig. 2d. As the channel vector is estimated more accurately than in the first step, the MRC detector has better performance. The

proposed joint channel estimation and data detection algorithm is illustrated in Fig. 2e.

IV. SIMULATION RESULTS

In this section, we evaluate the performance of the proposed channel estimation method and compare it to the EP scheme in terms of BER, NMSE, PAPR, and overhead. The system operates at a carrier frequency of $f_c = 4$ GHz and a subcarrier spacing of $\Delta f = 15$ kHz, with a maximum speed of the fading channel set to $v = 500$ km/h. The EVA channel model and Jakes' formula are used to generate DD channel parameters [9]. In this research, we assume that the delay and Doppler of each tap are integers. The pilot value in the EP scheme is $\sqrt{(4k_{max} + 1)(2l_{max} + 1)}$, and the dedicated pilot power to our method is lower than that of EP since we consider less pilot overhead. To simulate BER and NMSE curve, the parameter M and N are set to 64.

Fig. 3a shows the NMSE versus SNR for the proposed estimation method and EP. It can be seen that our proposed method in the first step cannot reach the EP performance. However, in the second step of the proposed method, the estimation error is much lower than that of EP for high SNRs. In low SNRs, the NMSE of the second step is worse than EP, which is due to the poor channel estimation in the first step resulting in inadequate data detection.

Fig. 3b illustrates the BER performance versus SNR, showing that the BER of the second step is the same as that of the EP and known CSI. Although the NMSE of the first step channel estimation does not reach EP, its BER is close to EP.

Fig. 4a shows the complementary cumulative distribution function (CCDF) for the PAPR of the transmitted signal for different M and N . It can be observed that the PAPR of the proposed method is much lower than that of the EP signal. This is because only one high power single pulse in the DD domain is used in the EP scheme. By increasing the number of M and N , the channel parameters l_{max} and k_{max} increase, respectively, resulting in an increase in the power dedicated to a single pilot in the EP scheme, and hence, high PAPR. However, in our proposed system, the pilots are spread in the DD domain, resulting in a low PAPR that changes slightly by increasing M and N .

Fig. 4b shows the number of overhead bins for the proposed method and EP scheme for different M and N . It can be observed that for large N , the overhead of the system increases. Since the pilot overhead in the EP scheme depends on k_{max} and our proposed method does not, by increasing N , the pilot overhead for the EP scheme increases dramatically compared to the proposed method.

V. CONCLUSION

In this paper, we propose a two-step joint channel estimation and data detection scheme for ZP-OTFS systems based on sparse recovery algorithms. In the first step, we use the OMP algorithm for channel estimation, and in the second step, we perform data detection using the MRC detector. Our proposed method offers significant improvements in both spectral and power efficiency while imposing a low PAPR on the transmitter.

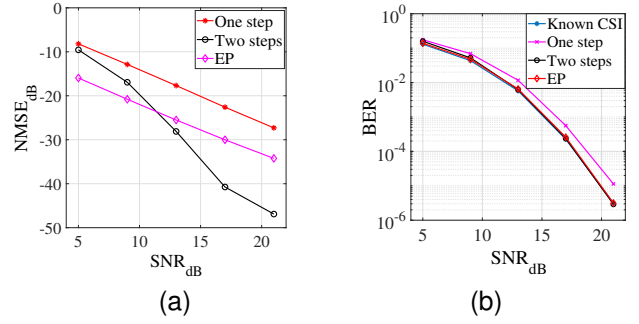


Fig. 3. (a) The NMSE of the proposed method (first step and second step) with EP, (b) The BER performance of proposed method with EP and known CSI.

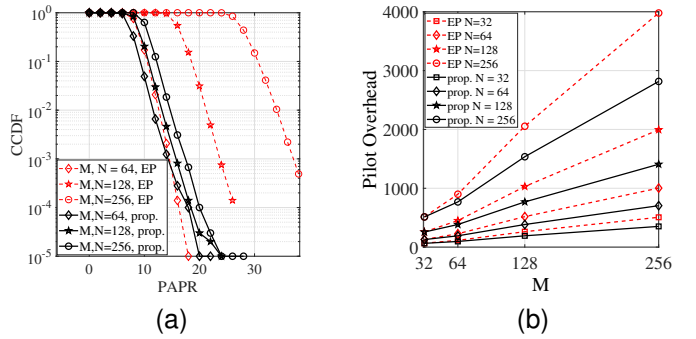


Fig. 4. (a) CCDF versus PAPR of the transmitted signal, (b) Number of pilot overhead versus M for different N .

REFERENCES

- [1] R. Hadani, S. Rakib, M. Tsatsanis, A. Monk, A. J. Goldsmith, A. F. Molisch, and R. Calderbank, "Orthogonal time frequency space modulation," *IEEE Wireless Communications and Networking Conference, WCNC*, 2017.
- [2] S. Tiwari, S. Sekhar Das, and V. Rangamgari, "low complexity lmmse receiver for OTFS," *IEEE communication letter*, vol. 23, no. 12, pp. 2205–2209.
- [3] P. Raviteja, K. T. Phan, Y. Hong, and E. Viterbo, "Interference cancellation and iterative detection for orthogonal time frequency space modulation," *IEEE Transactions on Wireless Communications*, vol. 17, no. 10, pp. 6501–6515, 2018.
- [4] T. Thaj and E. Viterbo, "Low Complexity Iterative Rake Decision Feedback Equalizer for Zero-Padded OTFS Systems," *IEEE Transactions on Vehicular Technology*, vol. 69, no. 12, pp. 15 606–15 622, 2020.
- [5] P. Raviteja, K. T. Phan, and Y. Hong, "Embedded Pilot-Aided Channel Estimation for OTFS in Delay-Doppler Channels," *IEEE Transactions on Vehicular Technology*, vol. 68, no. 5, pp. 4906–4917, 2019.
- [6] L. Zhao, W. Gao, and W. Guo, "sparse bayesian learning of delay doppler channel for otfs system," *IEEE Communication Letters*, vol. 24, no. 12, pp. 2766–2769.
- [7] H. B. Mishra, P. Singh, A. K. Prasad, and R. Budhiraja, "OTFS Channel Estimation And Data Detection Designs With Superimposed Pilots," *IEEE Transactions on Wireless Communications*, vol. 21, no. 4, pp. 2258–2274, 2021.
- [8] P. Raviteja, Y. Hong, E. Viterbo, and E. Biglieri, "Practical pulse-shaping waveforms for reduced-cyclic-prefix OTFS," *IEEE Transactions on Vehicular Technology*, vol. 68, no. 1, pp. 957–961, 2019.
- [9] Y. Hong, T. Thaj, and E. Viterbo, *Delay-Doppler Communication*, 2022, vol. 1, no. December.